Supplementary Information:

Hydroclimate variability of north western Amazon Basin in the Andes foothills in Peru during the last 1600 years

Analytical Methods

Age determinations were carried out at the Minnesota Isotope Laboratory (USA), using multi-collector inductively coupled plasma mass spectrometry technique (MC-ICP-MS, Thermo-Finnigan NEPTUNE), according to the procedures described in Cheng et al., (2013). Twenty samples weighing between 150 and 300 mg were dissolved and equilibrated with a ^{236}U-^{233}U-^{229}Th spike and then separated and purified using methods described in Edwards et al. (1987). Initial ^{230}Th values were corrected with a typical bulk earth ratio, i.e. atomic ratio of $^{230}Th/^{232}Th = 4.4 \pm 2.2$ ppm. U-Th isotopic data and ages are shown in Supplemental Table S1.

Oxygen isotope ratios are expressed in δ notation, the per mil deviation from the VPDB standard. For example for oxygen, $\delta^{18}O = [((^{18}O/^{16}O)\ sample/\ (^{18}O/^{16}O)VPDB) - 1] \times 1000$. For each measurement in PAL4 speleothem, approximately 200 μg of powder was drilled from the sample and analyzed with an on-line, automated, carbonate preparation system linked to a Finnigan Delta Plus Advantage. The speleothem reproducibility of standard materials is 0.1‰ for $\delta^{18}O$. For each measurement in PAL3 speleothem, ≤20 μg of powder was drilled and analyzed using a Kiel IV carbonate device coupled to a MAT 253 mass spectrometer (Thermo Finningan) allowing analytical precision around ± 0.04 ‰ for $\delta^{13}C$ e ± 0.08 ‰ for $\delta^{18}O$. Both samples were analyzed in the *Laboratório de estudos Geodinamicos e Ambientais* at the University of Brasilia (UnB).

Figure S1:

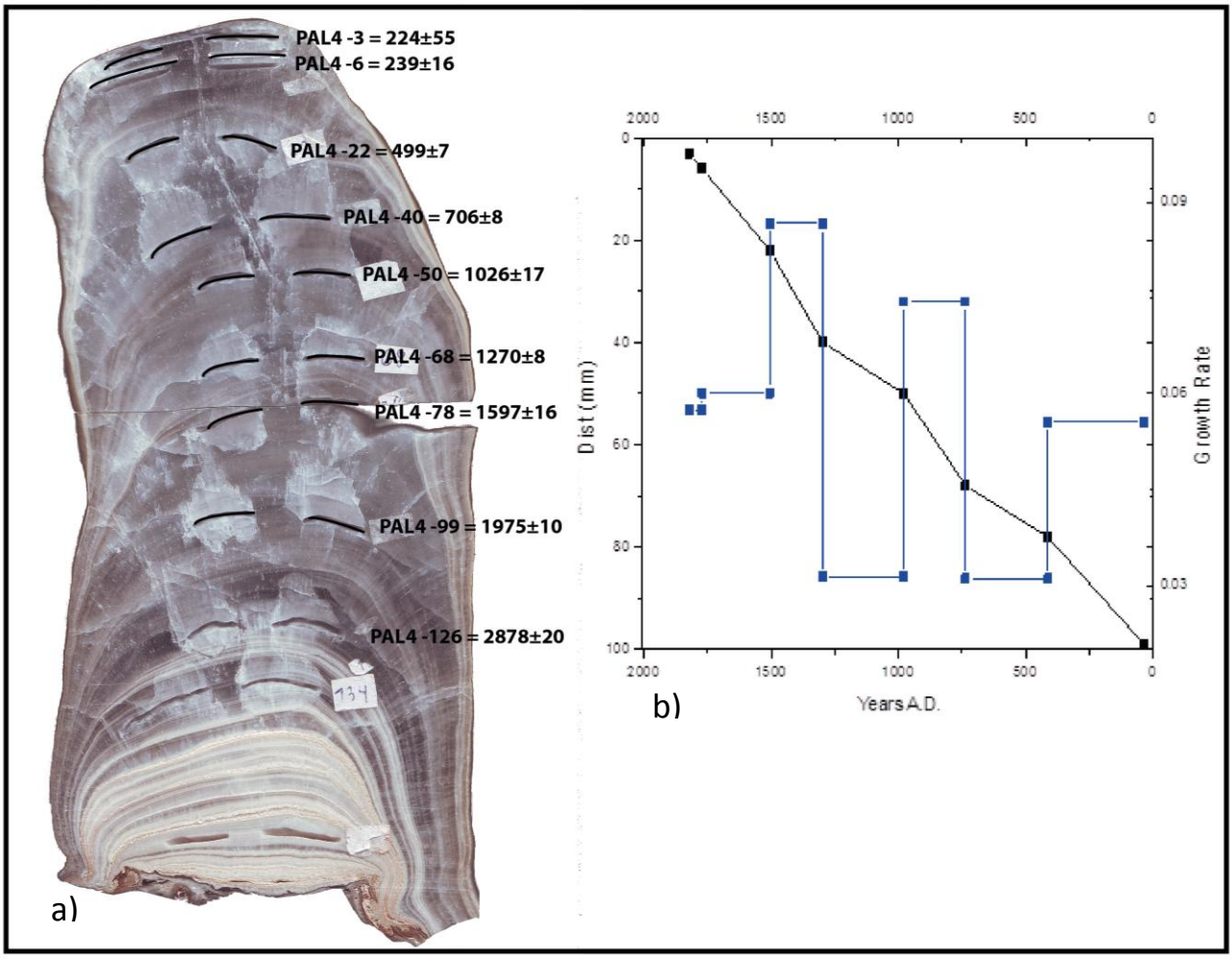

Figure S1: a) Pal4 Speleothem and respective location of U-Th dates along the sample. b) Growth Rate (Blue Lines) and Chronological model developed for the sample based on linear interpolation between dates (Black Line).

Figure S2:

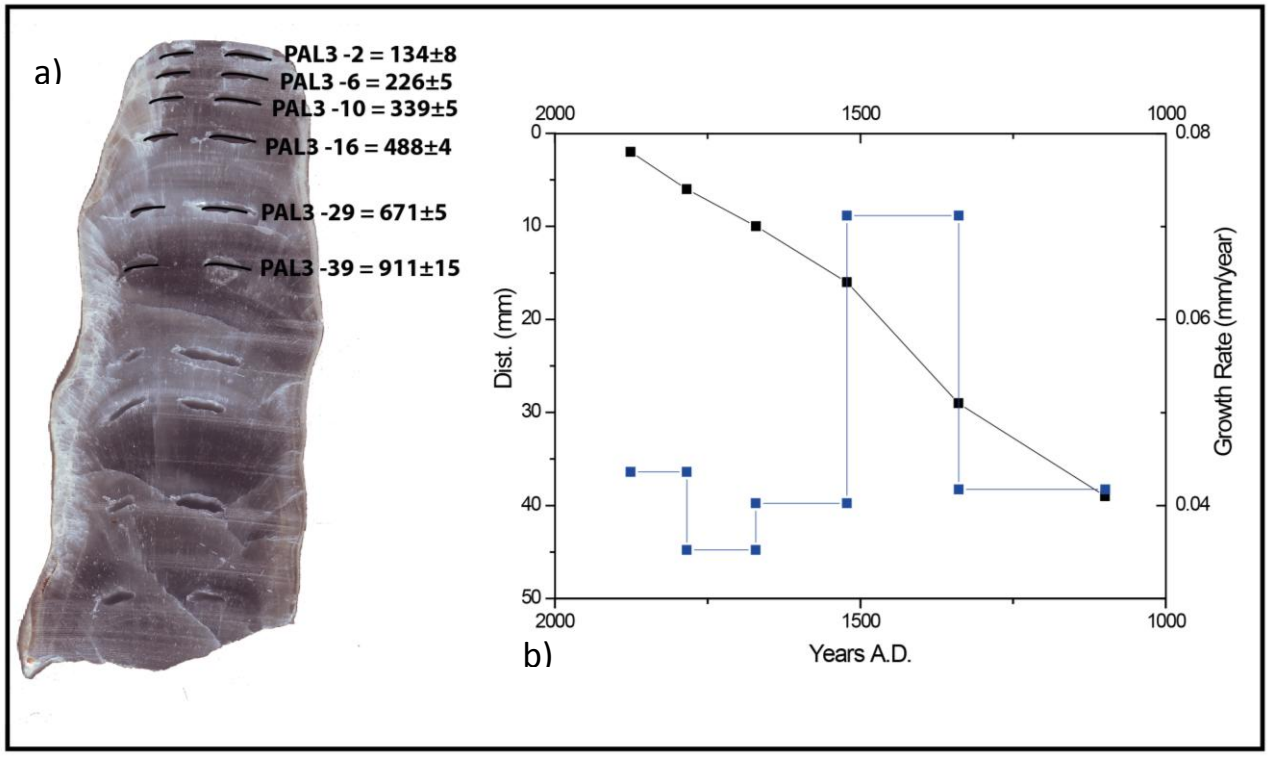

Figure S2: a) Pal3 Speleothem and respective location of U-Th dates along the sample. b) Growth Rate (Blue Lines) and Chronological model developed for the sample based on linear interpolation between dates (Black Line).

Figure S3

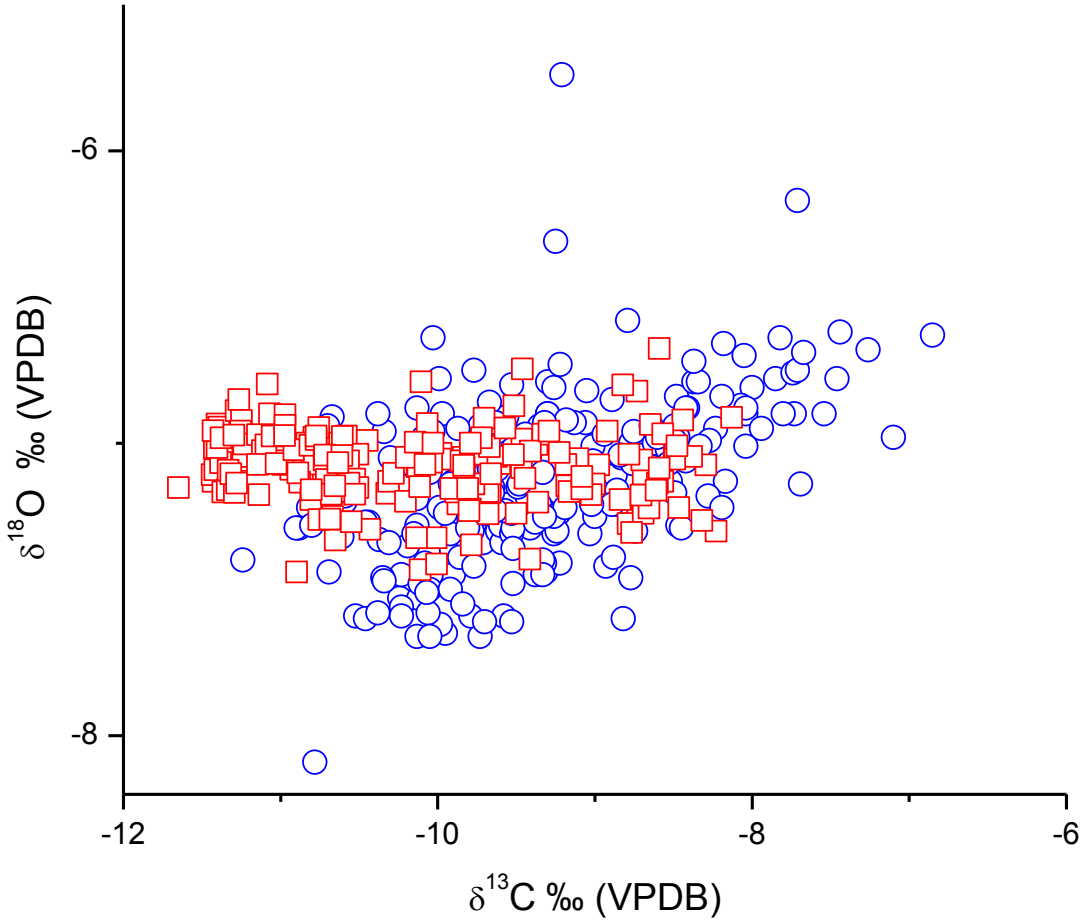

Figure S3: Scatter diagram of $\delta^{18}O$ versus $\delta^{13}C$ values for each analyzed stalagmite: blue circles indicate PAL4 stalagmite and red squares show PAL3 stalagmite.

Pal 4, R^2= 0.26 Pal 3, R^2 = 0.009

Figure S4

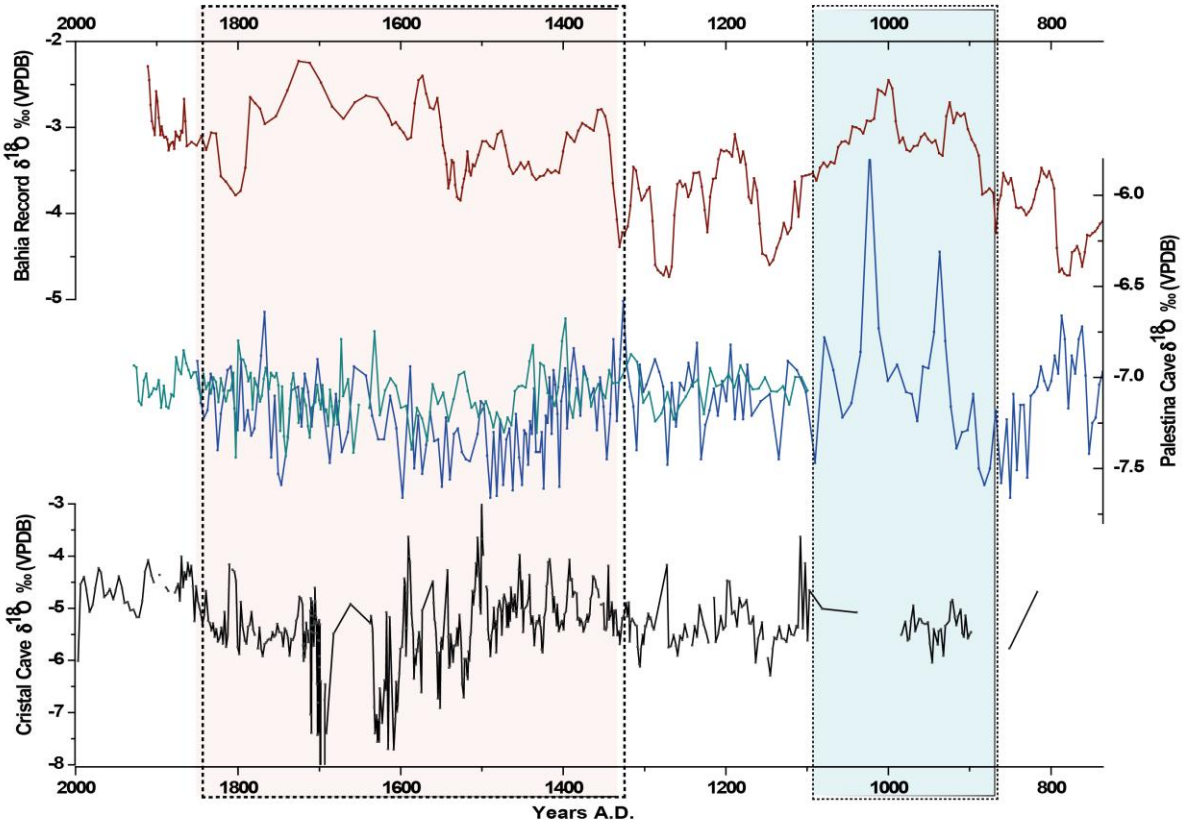

Figure S4: Comparison between Palestina cave $\delta^{18}O$ record (Blue and Cyan Line) and other high resolution proxies of the SAMS far from the Andes cordillera: In northeast South America, "Bahia Cave $\delta^{18}O$ record" (Red Line) (Novello et al, 2012) and South East South America, "Crystal Cave $\delta^{18}O$ record" (Black Line) (Taylor et al, 2010).

Figure S5

Spectral Analyses

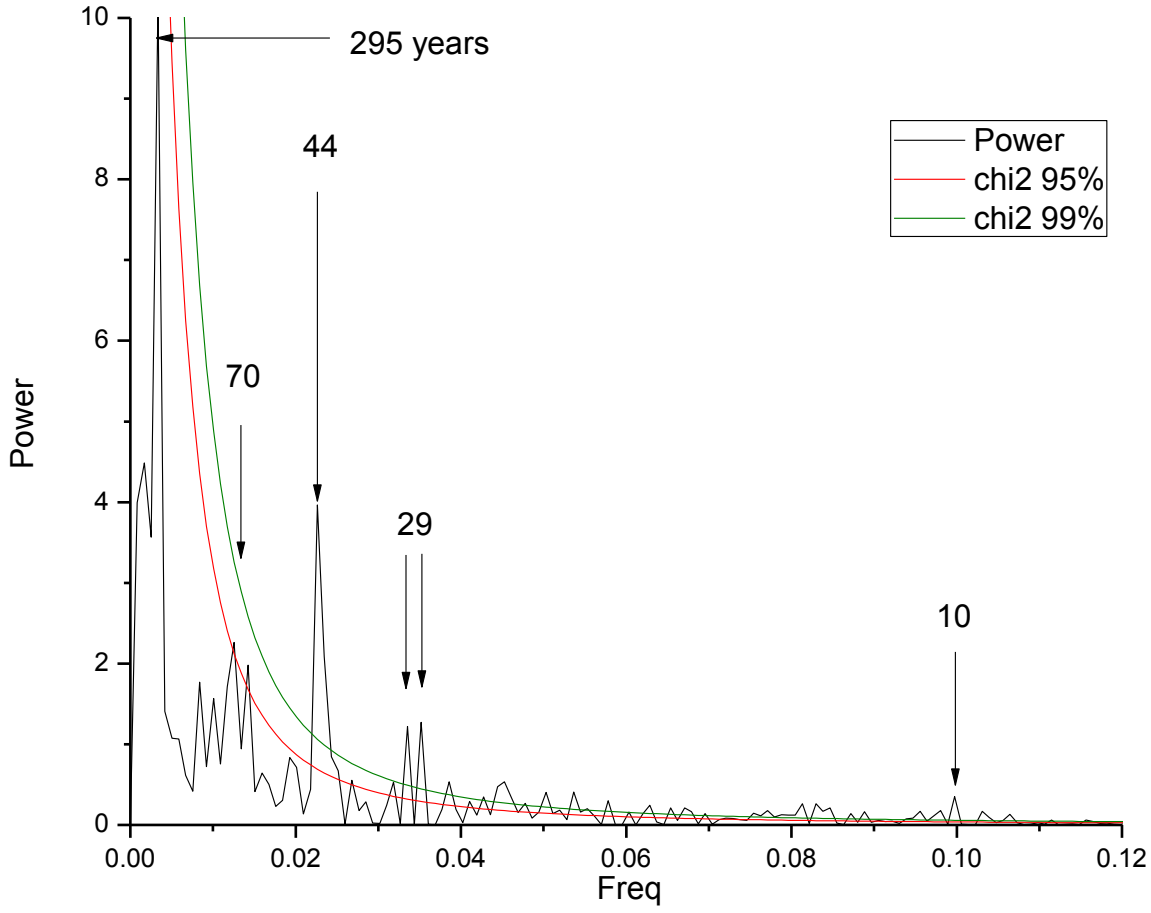

Figure S5: Spectral analysis of the $\delta^{18}O$ time series of palestina record. Peaks that exceed the 90 % confidence level are labeled with their periods (in years). Analyses were performed with the Past software (Hammer et al., 2001) using the same routine of Schulz and Mudelsee, (2002), which uses the Lomb-Scargle periodogram for unevenly spaced data.

Figure S6

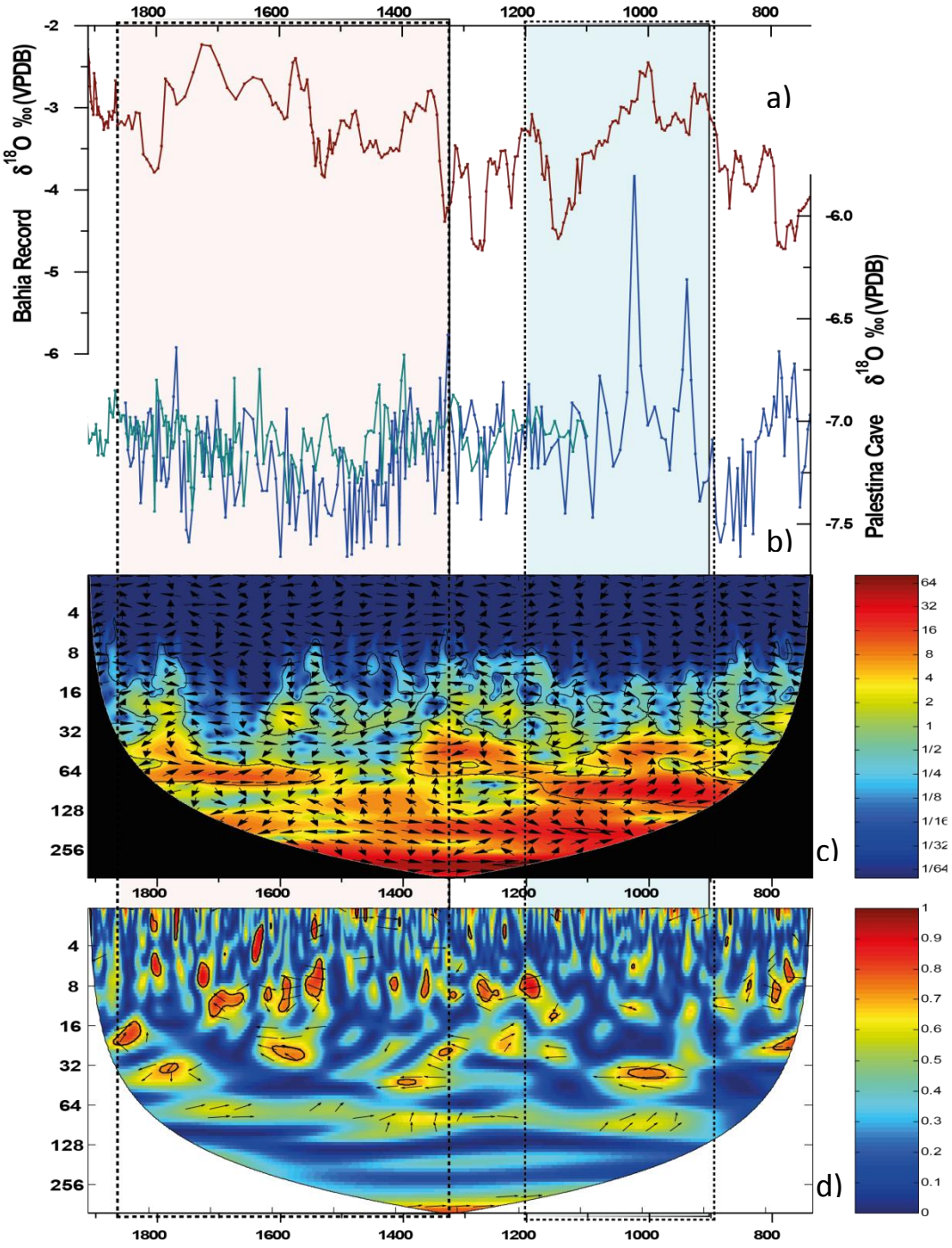

Figure S6: a) Northeastern South America record, (DV-2 record; Novello et al, 2012); b) Palestina cave record, c) Cross Wavelet analyses between both series; d) Coherence analyses between both series representing periods of similar periodicities.

Table S1

^{230}Th dating results. The error is 2σ error.

Sample Number	^{238}U (ppb)		^{232}Th (ppt)		^{230}Th / ^{232}Th (atomic x10^{-6})		δ^{234}U* (measured)		^{230}Th / ^{238}U (activity)		^{230}Th Age (yr) (uncorrected)		^{230}Th Age (yr) (corrected)	
PAL4-3	181	±0.4	1575	±32	17	±1	2271	±4	0.0090	±0.0002	301	±7	**224**	**±055**
PAL4-6	93.9	±0.1	131	±3	89	±5	2283.3	±3.1	0.0075	±0.0004	251	±14	**239**	**±16**
PAL4-11	230.0	±0.7	293	±6	122.2	±8.9	2306.2	±7.9	0.00943908	±0.00066	312	±22	**300**	**±23**
PAL4-16	422.5	±0.7	307	±7	285.6	±11.3	2289.2	±4.2	0.012608153	±0.00042	419	±14	**412**	**±15**
PAL4-22	349	±1.1	316	±6	279	±6	2293	±6	0.0153	±0.0001	507	±4	**499**	**±007**
PAL4-26	335.0	±0.9	231	±5	408.3	±13.1	2296.9	±6.6	0.017067833	±0.00041	566	±14	**560**	**±14**
PAL4-33	281.0	±0.9	144	±4	599.5	±25.8	2284.7	±7.8	0.018617254	±0.00064	619	±21	**615**	**±21**
PAL4-40	309	±0.5	288	±6	381	±8	2301	±5	0.0216	±0.0001	714	±5	**706**	**±008**
PAL4-46	220.9	±0.6	88	±3	1051.8	±40.7	2298.7	±6.9	0.025492211	±0.00063	845	±21	**842**	**±21**
PAL4-50	277	±0.4	692	±14	208	±4	2296	±4	0.0316	±0.0002	1048	±8	**1,026**	**±017**
PAL4-57	325.0	±1.0	278	±6	675	±18	2297.2	±8.1	0.035023	±0.0006	1163	±19	**1156**	**±20**
PAL4-68	360	±0.5	289	±6	790	±16	2294	±5	0.0384	±0.0002	1277	±6	**1,270**	**±008**
PAL4-78	94.7	±0.2	223	±5	341	±7	2302.9	±7.4	0.0487	±0.0004	1617	±14	**1597**	**±20**

*$\delta^{234}U = ([^{234}U/^{238}U]_{activity} - 1)x1000$.

** $\delta^{234}U_{initial}$ was calculated based on ^{230}Th age (T), i.e., $\delta^{234}U_{initial} = \delta^{234}U_{measured} \times e^{\lambda 234 \times T}$.

Corrected ^{230}Th ages assume the initial $^{230}Th/^{232}Th$ atomic ratio of 4.4 ±2.2 x10^{-6}. Those are the values for a material at secular equilibrium, with the bulk earth $^{232}Th/^{238}U$ value of 3.8. The errors are arbitrarily assumed to be 50%.

Table S2

^{230}Th dating results. The error is 2σ error.

Sample Number	^{238}U (ppb)		^{232}Th (ppt)		^{230}Th / ^{232}Th (atomic x10^{-6})		δ^{234}U* (measured)		^{230}Th / ^{238}U (activity)		^{230}Th Age (yr) (uncorrected)		^{230}Th Age (yr) (corrected)	
PAL3-2	474	±1.1	499	±10	67	±3	2269.5	±5.0	0.0043	±0.0001	143	±5	**134**	**±8**
PAL3-6	442.2	±1.1	185	±4	271	±8	2273.7	±5.2	0.0069	±0.0001	229	±5	**226**	**±5**
PAL3-10	471.2	±1.2	149	±4	532	±14	2265.7	±5.5	0.0102	±0.0001	342	±4	**339**	**±5**
PAL3-16	497.6	±1.3	126	±3	952	±24	2264.5	±5.0	0.0147	±0.0001	491	±4	**488**	**±4**
PAL3-29	488.4	±1.3	78	±2	2065	±59	2264.5	±5.2	0.0201	±0.0001	672	±5	**671**	**±5**
PAL3-39	122	±0.4	16	±1	3403	±203	2268.6	±5.4	0.0272	±0.0004	912	±15	**911**	**±15**

*$\delta^{234}U = ([^{234}U/^{238}U]_{activity} - 1)x1000$.

** $\delta^{234}U_{initial}$ was calculated based on ^{230}Th age (T), i.e., $\delta^{234}U_{initial} = \delta^{234}U_{measured} \times e^{\lambda 234 \times T}$.

Corrected ^{230}Th ages assume the initial $^{230}Th/^{232}Th$ atomic ratio of 4.4 ±2.2 x10^{-6}. Those are the values for a material at secular equilibrium, with the bulk earth $^{232}Th/^{238}U$ value of 3.8. The errors are arbitrarily assumed to be 50%.

References cited

Cheng, H., Edwards, R. L., Shen, C., Polyak, V. J., Asmerom, Y., Woodhead, J., Hellstrom,. Wang, Y., Kong, X., Spötl, C., Wang, X., Alexander C.J.: Improvements in ^{230}Th dating, ^{230}Th and ^{234}U half-life values , and U – Th isotopic measurements by multi-collector inductively coupled plasma mass spectrometry. Earth Planet. Sc. Lett., 371-372, 82–91. doi:10.1016/j.epsl.2013.04.006, 2013.

Edwards, R.L., Chen, J.H., and Wasserburg, G.J.: ^{238}U–^{234}U–^{230}Th–^{232}Th systematics and the precise measurement of time over the past 500,000 years: Earth Planet. Sc. Lett., 81, 175–192, 1987.

Hammer, Ø., Harper, D.A.T., Ryan, P.D., 2001, PAST: Paleontological Statistics Software Package for Education and Data Analysis: Palaeontologia Electronica v. 4, 9. http://palaeo-electronica.org/2001_1/past/issue1_01.htm.

Haug, G., Hughen, K., Sigman, D.M., Peterson, L.C., Röhl, U.: Southward migration of the Intertropical Convergence Zone through the Holocene, Science, 293, 1304-1308, 2001.

Shen, C-C., Edwards, R. L., Cheng, H., Dorale, J. A., Thomas, R. B., Moran, S. B., Weinstein, S. E., Edmonds H. N.: Uranium and thorium isotopic and concentration measurements by magnetic sector inductively coupled plasma mass spectrometry, Chem. Geol., 185, 165-178, 2002.

Shulz, M.; Mudelsse, M.: REDFIT: estimating red-noise spectra directly from unevenly spaced paleoclimatic time series: Computers & Geosciences, v. 28, p. 421–426, 2002.

Torrence, C., Compo, G.P.: A Practical Guide to Wavelet Analysis: B. Am. Meteorol. Soc., 79, 61-78, 1998.

Wang, Y., Cheng, H., Edwards, R.L., He, Y., Kong, X. An, Z., Wu, J., Kelly, M. J., Dykoski, C. A., Li, X.:The Holocene Asian Monsoon: Links to solar changes and North Atlantic climate, Science, 308, 854-857, doi: 10.1126/science.1106296, 2005.